



Contents lists available at ScienceDirect

## Journal of Nuclear Materials

journal homepage: [www.elsevier.com/locate/jnucmat](http://www.elsevier.com/locate/jnucmat)

## Thermodynamic assessments of the Al–Th and Th–Zn systems

Z.S. Li<sup>a</sup>, X.J. Liu<sup>a</sup>, M.Z. Wen<sup>a</sup>, C.P. Wang<sup>a,\*</sup>, A.T. Tang<sup>b</sup>, F.S. Pan<sup>b</sup><sup>a</sup> Department of Materials Science and Engineering, College of Materials, and Research Center of Materials Design and Applications, Xiamen University, Xiamen 361005, PR China<sup>b</sup> College of Materials Science and Engineering, Chongqing University, Chongqing 400045, PR China

## ARTICLE INFO

## Article history:

Received 8 August 2009

Accepted 31 October 2009

## Keywords:

Nuclear reactor materials

Phase diagrams

Thermodynamic modeling

## ABSTRACT

The phase diagrams of the Al–Th and Th–Zn systems have been evaluated by using the Calculation of Phase Diagrams (CALPHAD) method with the experimental data including the phase equilibria and thermodynamic properties. The Gibbs free energies of the liquid, bcc and hcp phases were described by the subregular solution model with the Redlich–Kister equation, and those of the stoichiometric compounds of the Th<sub>2</sub>Al, Th<sub>3</sub>Al<sub>2</sub>, ThAl, Th<sub>2</sub>Al<sub>3</sub>, ThAl<sub>2</sub>, ThAl<sub>3</sub>, Th<sub>2</sub>Al<sub>7</sub>, Th<sub>2</sub>Zn, ThZn<sub>2</sub>, ThZn<sub>4</sub> and Th<sub>2</sub>Zn<sub>17</sub> were described by the two-sublattice model. The calculated phase equilibria and thermodynamic properties are in good agreement with the experimental data.

© 2009 Elsevier B.V. All rights reserved.

## 1. Introduction

Nuclear energy is a new kind of important energy, and the nuclear materials are the important fundamental guarantee to develop a safe nuclear reactor with high efficiency [1–3]. Thorium (Th) is an abundant element in nature with multiple advantages as a nuclear fuel for future reactors of all types [4]. The traditional methods of materials researches with many experimental tries are unsuitable in the nuclear materials researches because of the rigorous experimental conditions. Thus, the investigation on the phase diagrams of nuclear materials systems is very important for development of new nuclear materials. Our goal is to develop the thermodynamic database of the phase diagrams in nuclear material system. The present authors have made some thermodynamic assessments of nuclear material system [5–11]. As a part of this thermodynamic database, the purpose of the present work is to carry out thermodynamic assessment of the phase diagrams in the Al–Th and Th–Zn systems based on the Calculation of Phase Diagrams (CALPHAD) method by means of the available experimental data.

## 2. Thermodynamic models

The information of the stable solid phases and the used models in the Al–Th and Th–Zn systems are presented in Table 1.

## 2.1. Solution phases

Gibbs free energies of the solution phases (liquid, hcp, fcc and bcc phases) in an A–B system, corresponding to the Al–Th, and Th–Zn systems, are described by the subregular solution model. The molar Gibbs free energy of each solution phase in A–B system is given as follows:

$$G_m^\phi = \sum_{i=A,B} {}^0G_i^\phi x_i + RT \sum_{i=A,B} x_i \ln x_i + {}^E G_m^\phi, \quad (1)$$

where  ${}^0G_i^\phi$  is the molar Gibbs free energy of pure component  $i$  in the respective reference state with the  $\phi$  phase, which is taken from the SGTE pure element database [12].  $R$  is the gas constant, and  $T$  is the absolute temperature. The  $x_i$  denotes the mole fraction of component  $i$ . The term  ${}^E G_m^\phi$  is the excess Gibbs free energy, which is expressed in the Redlich–Kister polynomials [13] as:

$${}^E G_m^\phi = L_{A,B}^\phi x_A x_B, \quad (2)$$

where  $L_{A,B}^\phi$  is the interaction energies in a hypothetical binary system denoted by A–B, which is expressed in the following forms:

$$\begin{aligned} L_{A,B}^\phi &= {}^0L_{A,B}^\phi + {}^1L_{A,B}^\phi(x_A - x_B) + {}^2L_{A,B}^\phi(x_A - x_B)^2 + \dots \\ &= \sum_{m=0}^n {}^mL_{A,B}^\phi(x_A - x_B)^m, \end{aligned} \quad (3)$$

$${}^mL_{A,B}^\phi = a + bT, \quad (4)$$

where the parameters of  $a$  and  $b$  were evaluated based on the experimental data in binary systems, respectively.

\* Corresponding author. Tel.: +86 592 2180606; fax: +86 592 2187966.  
E-mail address: [wangcp@xmu.edu.cn](mailto:wangcp@xmu.edu.cn) (C.P. Wang).

**Table 1**

The stable solid phases and the used models in the Al–Th and Th–Zn systems.

| System                           | Phase                           | Prototype                        | Crystal system | Modeling phase                              | Used models |     |
|----------------------------------|---------------------------------|----------------------------------|----------------|---|-------------|-----|
| Th–Al                            | $\alpha$ Th                     | Cu                               | fcc            | (Al, Th)                                    | SSM         |     |
|                                  | $\beta$ Th                      | W                                | bcc            | (Al, Th)                                    | SSM         |     |
|                                  | (Al)                            | Cu                               | fcc            | (Al, Th)                                    | SSM         |     |
|                                  | Th <sub>2</sub> Al              | Al <sub>2</sub> Cu               | bct            | (Th) <sub>0.667</sub> (Al) <sub>0.333</sub> | SM          |     |
|                                  | Th <sub>3</sub> Al <sub>2</sub> | U <sub>3</sub> Si <sub>2</sub>   | Tetragonal     | (Th) <sub>0.6</sub> (Al) <sub>0.4</sub>     | SM          |     |
|                                  | ThAl                            | CrB                              | Orthorhombic   | (Th) <sub>0.5</sub> (Al) <sub>0.5</sub>     | SM          |     |
|                                  | Th <sub>2</sub> Al <sub>3</sub> | –                                | Tetragonal     | (Th) <sub>0.4</sub> (Al) <sub>0.6</sub>     | SM          |     |
|                                  | ThAl <sub>2</sub>               | AlB <sub>2</sub>                 | Hexagonal      | (Th) <sub>0.333</sub> (Al) <sub>0.667</sub> | SM          |     |
|                                  | ThAl <sub>3</sub>               | SnNi <sub>3</sub>                | Hexagonal      | (Th) <sub>0.25</sub> (Al) <sub>0.75</sub>   | SM          |     |
|                                  | Th <sub>2</sub> Al <sub>7</sub> | –                                | Orthorhombic   | (Th) <sub>0.222</sub> (Al) <sub>0.778</sub> | SM          |     |
|                                  | Th–Zn                           | $\alpha$ Th                      | Cu             | fcc   | (Th, Zn)    | SSM |
|                                  |                                 | $\beta$ Th                       | W              | bcc   | (Th, Zn)    | SSM |
| (Zn)                             |                                 | Mg                               | hcp            | (Th, Zn)                                    | SSM         |     |
| Th <sub>2</sub> Zn               |                                 | Al <sub>2</sub> Cu               | bct            | (Th) <sub>0.667</sub> (Zn) <sub>0.333</sub> | SM          |     |
| ThZn <sub>2</sub>                |                                 | –                                | Hexagonal      | (Th) <sub>0.333</sub> (Zn) <sub>0.667</sub> | SM          |     |
| ThZn <sub>4</sub>                |                                 | BaAl <sub>4</sub>                | bct            | (Th) <sub>0.2</sub> (Zn) <sub>0.8</sub>     | SM          |     |
| Th <sub>2</sub> Zn <sub>17</sub> |                                 | Th <sub>2</sub> Zn <sub>17</sub> | Rhombohedral   | (Th) <sub>0.105</sub> (Zn) <sub>0.895</sub> | SM          |     |

SSM: subregular solution model and SM: sublattice model.

## 2.2. Stoichiometric intermetallic compounds

In the Th–Me (Me: Al or Zn) system, the intermetallic compounds (Th<sub>2</sub>Al, Th<sub>3</sub>Al<sub>2</sub>, ThAl, Th<sub>2</sub>Al<sub>3</sub>, ThAl<sub>2</sub>, ThAl<sub>3</sub>, Th<sub>2</sub>Al<sub>7</sub>, Th<sub>2</sub>Zn, ThZn<sub>2</sub>, ThZn<sub>4</sub> and Th<sub>2</sub>Zn<sub>17</sub>) are stoichiometric compounds. The Gibbs free energy for per mole of formula unit Th<sub>p</sub>Me<sub>q</sub> can be expressed as:

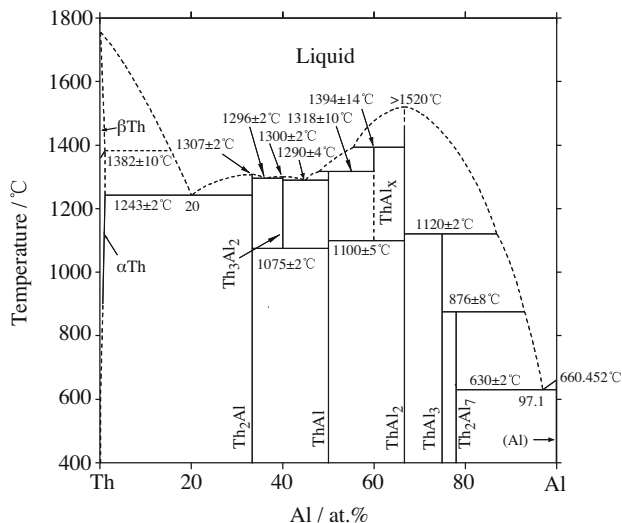
$$\Delta^0 G_f^{\text{Th}_p\text{Me}_q} = G_m^{\text{Th}_p\text{Me}_q} - p^0 G_{\text{Th}}^{\text{ref}} - q^0 G_{\text{Me}}^{\text{ref}} = a' + b'T, \quad (5)$$

where the  $\Delta^0 G_f^{\text{Th}_p\text{Me}_q}$  indicates the standard Gibbs free energy for the formation of the stoichiometric compound from pure elements, and the parameters of  $a'$  and  $b'$  were evaluated in the present paper.

## 3. Experimental information

### 3.1. The Al–Th binary system

The phase diagram in the Al–Th system consists of four solution phases (liquid,  $\alpha$ Th,  $\beta$ Th, (Al) phases), and seven intermetallic compounds (Th<sub>2</sub>Al, Th<sub>3</sub>Al<sub>2</sub>, ThAl, Th<sub>2</sub>Al<sub>3</sub>, ThAl<sub>2</sub>, ThAl<sub>3</sub>, Th<sub>2</sub>Al<sub>7</sub> phases). The phase diagram in the Al–Th system has been investigated by many researchers [14–19]. Murray [17] studied the phase diagram

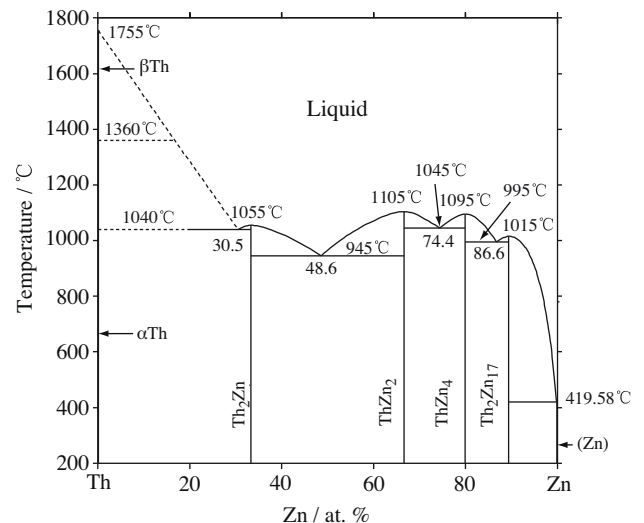
**Fig. 1.** The phase diagram of the Al–Th system reviewed by Kassner [20].

in the Al–Th system by thermal analysis, X-ray diffraction and metallographic methods, and found that the Th<sub>2</sub>Al, Th<sub>3</sub>Al<sub>2</sub> and ThAl<sub>2</sub> compounds are directly formed from the liquid phase, while the ThAl, Th<sub>2</sub>Al<sub>3</sub> and ThAl<sub>3</sub> compounds are formed by the peritectic reactions (Th<sub>2</sub>Al<sub>3</sub> + L  $\leftrightarrow$  ThAl, L + ThAl<sub>2</sub>  $\leftrightarrow$  Th<sub>2</sub>Al<sub>3</sub> or L + ThAl<sub>2</sub>  $\leftrightarrow$  ThAl<sub>3</sub>). Murray [17] reported that the Th<sub>3</sub>Al<sub>2</sub> and Th<sub>2</sub>Al<sub>3</sub> compounds eutectoidally decompose at 1075 °C and 1100 °C, respectively, and the solid solubilities of Al in the  $\alpha$ Th and  $\beta$ Th phases are 0.4 at.% at 1000 °C and 0.85 at.% at 1300 °C. However, the liquidus of the Al–Th binary system around the Th-corner has not been determined. The phase diagram in the Al–Th system reviewed by Kassner et al. [20] is shown in Fig. 1.

In addition, the enthalpies and entropies of formation of the Th<sub>2</sub>Al<sub>7</sub> and ThAl<sub>3</sub> compounds in the temperature range from 673 °C to 807 °C were determined by Poyarkov et al. [19] on the basis of Electromotive Force (EMF) measurements. And the enthalpy formation of ThAl<sub>2</sub> was measured calorimetrically by Wang et al. [21].

### 3.2. The Th–Zn binary system

The phase diagram in the Th–Zn system consists of four solution phases (liquid,  $\alpha$ Th,  $\beta$ Th, (Zn) phases), and four intermetallic

**Fig. 2.** The phase diagram of the Th–Zn system reviewed by Okamoto [27].

compounds ( $\text{Th}_2\text{Zn}$ ,  $\text{ThZn}_2$ ,  $\text{ThZn}_4$ ,  $\text{Th}_2\text{Zn}_{17}$  phases). The phase diagram in the Th–Zn system was investigated by many researchers [22–26]. Chiotti and Gill [26] determined the phase diagram in the Th–Zn system by thermal analysis, metallographic method

**Table 2**  
Thermodynamic parameters in the Al–Th system.

| System  | Parameters in each phase (J/mol)   |
|---|--|
| Th–Al   | Liquid phase, format (Al, Th) <sub>1</sub>   |
|   | ${}^0L_{\text{Al,Th}}^{\text{Liq}} = -93725 + 4.523T$  |
|   | ${}^1L_{\text{Al,Th}}^{\text{Liq}} = -30000$   |
|   | ${}^2L_{\text{Al,Th}}^{\text{Liq}} = -20156 + 9.264T$  |
|   | Fcc phase (A1), format (Al, Th) <sub>1</sub> (Va) <sub>1</sub>   |
|   | ${}^0L_{\text{Al,Th}}^{\text{fcc}} = 6670$   |
|   | ${}^1L_{\text{Al,Th}}^{\text{fcc}} = 10557 + 7.000T$   |
|   | ${}^2L_{\text{Al,Th}}^{\text{fcc}} = -27932$   |
|   | Bcc phase (A2), format (Al, Th) <sub>1</sub> (Va) <sub>3</sub>   |
|   | ${}^0L_{\text{Al,Th}}^{\text{bcc}} = -32510$   |
|   | ${}^1L_{\text{Al,Th}}^{\text{bcc}} = 26059$  |
|   | ${}^2L_{\text{Al,Th}}^{\text{bcc}} = 20000$  |
|   | $\text{Th}_2\text{Al}$ phase, format (Th) <sub>0.6667</sub> (Al) <sub>0.3333</sub>   |
|   | $G_{\text{Al,Th}}^{\text{Th}_2\text{Al}} = -44333 + 11.491T + 0.6667^0G_{\text{Th}}^{\text{fcc}} + 0.3333^0G_{\text{Al}}^{\text{fcc}}$ |
|   | $\text{Th}_3\text{Al}_2$ phase, format (Th) <sub>0.6</sub> (Al) <sub>0.4</sub>   |
|   | $G_{\text{Al,Th}}^{\text{Th}_3\text{Al}_2} = -41970 + 7.999T + 0.6^0G_{\text{Th}}^{\text{fcc}} + 0.4^0G_{\text{Al}}^{\text{fcc}}$      |
|   | ThAl phase, format (Th) <sub>0.5</sub> (Al) <sub>0.5</sub>   |
|   | $G_{\text{Al,Th}}^{\text{ThAl}} = -42950 + 6.127T + 0.5^0G_{\text{Th}}^{\text{fcc}} + 0.5^0G_{\text{Al}}^{\text{fcc}}$                 |
|   | $\text{Th}_2\text{Al}_3$ phase, format (Th) <sub>0.4</sub> (Al) <sub>0.6</sub>   |
|   | $G_{\text{Al,Th}}^{\text{Th}_2\text{Al}_3} = -38940 + 1.719T + 0.4^0G_{\text{Th}}^{\text{fcc}} + 0.6^0G_{\text{Al}}^{\text{fcc}}$      |
| $\text{ThAl}_2$ phase, format (Th) <sub>0.3333</sub> (Al) <sub>0.6667</sub>   |  |
| $G_{\text{Al,Th}}^{\text{ThAl}_2} = -41518 + 2.593T + 0.3333^0G_{\text{Th}}^{\text{fcc}} + 0.6667^0G_{\text{Al}}^{\text{fcc}}$          |  |
| $\text{ThAl}_3$ phase, format (Th) <sub>0.25</sub> (Al) <sub>0.75</sub>   |  |
| $G_{\text{Al,Th}}^{\text{ThAl}_3} = -37826 + 4.805T + 0.25^0G_{\text{Th}}^{\text{fcc}} + 0.75^0G_{\text{Al}}^{\text{fcc}}$              |  |
| $\text{Th}_2\text{Al}_7$ phase, format (Th) <sub>0.2222</sub> (Al) <sub>0.7778</sub>  |  |
| $G_{\text{Al,Th}}^{\text{Th}_2\text{Al}_7} = -36911 + 6.698T + 0.2222^0G_{\text{Th}}^{\text{fcc}} + 0.7778^0G_{\text{Al}}^{\text{fcc}}$ |  |

**Table 3**  
Thermodynamic parameters in the Th–Zn system.

| System | Parameters in each phase (J/mol)   |
|--------|--|
| Th–Zn  | Liquid phase, format (Th, Zn) <sub>1</sub>   |
|        | ${}^0L_{\text{Th,Zn}}^{\text{Liq}} = -85000 + 17.000T$   |
|        | ${}^1L_{\text{Th,Zn}}^{\text{Liq}} = 50000$  |
|        | ${}^2L_{\text{Th,Zn}}^{\text{Liq}} = -50000 + 15.000T$   |
|        | Fcc phase (A1), format (Th, Zn) <sub>1</sub> (Va) <sub>1</sub>   |
|        | ${}^0L_{\text{Th,Zn}}^{\text{fcc}} = 20000$  |
|        | Bcc phase (A2), format (Th, Zn) <sub>1</sub> (Va) <sub>3</sub>   |
|        | ${}^0L_{\text{Th,Zn}}^{\text{bcc}} = 20000$  |
|        | Hcp phase (A3), format (Th, Zn) <sub>1</sub> (Va) <sub>0.5</sub>   |
|        | $G_{\text{Th}}^{\text{hcp}} = 5000 + G_{\text{Th}}^{\text{fcc}}$   |
|        | ${}^0L_{\text{Th,Zn}}^{\text{hcp}} = 0$  |
|        | $\text{Th}_2\text{Zn}$ phase, format (Th) <sub>0.6667</sub> (Zn) <sub>0.3333</sub>   |
|        | $G_{\text{Th,Zn}}^{\text{Th}_2\text{Zn}} = -18800 + 1.250T + 0.6667^0G_{\text{Th}}^{\text{fcc}} + 0.3333^0G_{\text{Zn}}^{\text{hcp}}$    |
|        | $\text{ThZn}_2$ phase, format (Th) <sub>0.3333</sub> (Zn) <sub>0.6667</sub>  |
|        | $G_{\text{Th,Zn}}^{\text{ThZn}_2} = -32180 + 2.400T + 0.3333^0G_{\text{Th}}^{\text{fcc}} + 0.6667^0G_{\text{Zn}}^{\text{hcp}}$           |
|        | $\text{ThZn}_4$ phase, format (Th) <sub>0.2</sub> (Zn) <sub>0.8</sub>  |
|        | $G_{\text{Th,Zn}}^{\text{ThZn}_4} = -28700 + 1.200T + 0.2^0G_{\text{Th}}^{\text{fcc}} + 0.8^0G_{\text{Zn}}^{\text{hcp}}$                 |
|        | $\text{Th}_2\text{Zn}_{17}$ phase, format (Th) <sub>0.105</sub> (Zn) <sub>0.895</sub>  |
|        | $G_{\text{Th,Zn}}^{\text{Th}_2\text{Zn}_{17}} = -26550 + 4.900T + 0.105^0G_{\text{Th}}^{\text{fcc}} + 0.895^0G_{\text{Zn}}^{\text{hcp}}$ |

and vapor pressure method, and found that the melting points of these compounds ( $\text{Th}_2\text{Zn}$ ,  $\text{ThZn}_2$ ,  $\text{ThZn}_4$  and  $\text{Th}_2\text{Zn}_{17}$ ) under constrained vapor conditions were 1055 °C, 1105 °C, 1095 °C and 1015 °C, respectively. Five eutectic reactions of the  $L \leftrightarrow \alpha\text{Th} + \text{Th}_2\text{Zn}$ ,  $L \leftrightarrow \text{ThZn}_2 + \text{ThZn}_4$ ,  $L \leftrightarrow \text{ThZn}_4 + \text{Th}_2\text{Zn}_{17}$ ,  $L \leftrightarrow \text{Th}_2\text{Zn} + \text{ThZn}_2$  and  $L \leftrightarrow \text{Th}_2\text{Zn}_{17} + \text{Zn}$  exist in this system with the following eutectic temperatures and Zn atom percentages: 1040 °C and 30.5 at.% Zn, 945 °C and 48.6 at.% Zn, 1045 °C and 74.4 at.% Zn, 995 °C and 86.8 at.% Zn, 419.58 °C and 0 at.% Zn. However, the relation between the liquid and Th-rich phases (including  $\alpha\text{Th}$  and  $\beta\text{Th}$  phases) was only estimated by Chiotti and Gill [26] without enough experimental data. The phase diagram in the Th–Zn system reviewed by Okamoto [27] is shown in Fig. 2.

In addition, the standard enthalpy and entropy of formation for the compounds in the Th–Zn system were determined by many researchers [26,28–30] using vapor pressure measurement or EMF method. Based on these experimental data, Chiotti et al. [31] calculated these thermodynamic properties of the  $\text{Th}_2\text{Zn}_{17}$ ,  $\text{ThZn}_4$ ,  $\text{ThZn}_2$  and  $\text{Th}_2\text{Zn}$  compounds.

#### 4. Optimized results and discussion

Optimization of thermodynamic parameters describing the Gibbs free energy of each phase is carried out by using PARROT module in the Thermo-Calc software [32], a computer program that can accept different types of data, such as any specific thermodynamic quantities and phase equilibria, in the same operation. Each piece of the selected data is given a certain weight and the weight can be changed until a satisfactory description for most of the selected data is achieved.

All the parameters were finally evaluated together and adjustments were made to give the best description of the binary Al–Th and Th–Zn systems. All evaluated parameters are listed in Tables 2 and 3.

##### 4.1. Al–Th system

Fig. 3 shows the calculated phase diagram in the Al–Th system compared with the experimental data [14,15,18,19], and all the invariant reactions in the Al–Th system are listed in Table 4, where good agreement between calculated results and experimental data is obtained. The deviation between the calculated liquidus and the

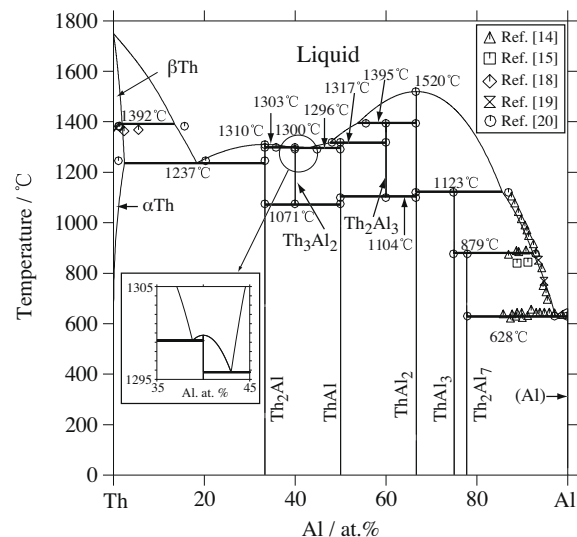


**Fig. 3.** The calculated phase diagram of the Al–Th system with the experimental data [14,15,18–20].

**Table 4**

Experimental and calculated invariant reactions in the Al–Th system.

| Reaction type       | Reaction  |      | Al (at.%) |      | T (°C)    | Reference |
|---------------------|---|------|-----------|------|-----------|-----------|
| Peritectic reaction | L + ThAl <sub>2</sub> ↔ Th <sub>2</sub> Al <sub>3</sub>     | 56   | 66.7      | 60   | 1394 ± 14 | [20]      |
|                     |   | 53.8 | 66.7      | 60   | 1394.8    | This work |
| Peritectic reaction | L + βTh ↔ αTh   | 15   | 1         | ~1   | 1382 ± 10 | [20]      |
|                     |   | 13.4 | 1.91      | 1.93 | 1391.8    | This work |
| Peritectic reaction | Th <sub>2</sub> Al <sub>3</sub> + L ↔ ThAl                  | 60   | 48        | 50   | 1318 ± 10 | [20]      |
|                     |   | 60   | 47.6      | 50   | 1317.3    | This work |
| Eutectic reaction   | L ↔ Th <sub>3</sub> Al <sub>2</sub> + Th <sub>2</sub> Al    | 35   | 40        | 33.3 | 1296 ± 2  | [20]      |
|                     |   | 38.8 | 40        | 33.3 | 1299.2    | This work |
| Eutectic reaction   | L ↔ ThAl + Th <sub>3</sub> Al <sub>2</sub>                  | 43   | 50        | 40   | 1290 ± 4  | [20]      |
|                     |   | 43   | 50        | 40   | 1295.8    | This work |
| Eutectic reaction   | L ↔ Th <sub>2</sub> Al + αTh                                | 20   | 33.3      | 0.85 | 1243 ± 2  | [20]      |
|                     |   | 18.3 | 33.3      | 2.4  | 1236.5    | This work |
| Peritectic reaction | L + ThAl <sub>2</sub> ↔ ThAl <sub>3</sub>                   | 84   | 66.7      | 75   | 1120 ± 2  | [20]      |
|                     |   | 85.6 | 66.7      | 75   | 1122.6    | This work |
| Eutectoid reaction  | Th <sub>2</sub> Al <sub>3</sub> ↔ ThAl <sub>2</sub> + ThAl  | 60   | 66.7      | 50   | 1100 ± 5  | [20]      |
|                     |   | 60   | 66.7      | 50   | 1104.1    | This work |
| Eutectoid reaction  | Th <sub>3</sub> Al <sub>2</sub> ↔ ThAl + Th <sub>2</sub> Al | 40   | 50        | 33.3 | 1075 ± 2  | [20]      |
|                     |   | 40   | 50        | 33.3 | 1070.9    | This work |
| Peritectic reaction | L + ThAl <sub>3</sub> ↔ Th <sub>2</sub> Al <sub>7</sub>     | 92.9 | 75        | 77.8 | 876 ± 8   | [20]      |
|                     |   | 92.4 | 75        | 77.8 | 879.2     | This work |
| Eutectic reaction   | L ↔ (Al) + Th <sub>2</sub> Al <sub>7</sub>                  | 97.1 | 0         | 77.8 | 630 ± 2   | [20]      |
|                     |   | 97.3 | 0         | 77.8 | 628.4     | This work |
| Congruent reaction  | L ↔ Th <sub>2</sub> Al                                      |      | 33.3      |      | 1307 ± 2  | [20]      |
|                     |   |      | 33.3      |      | 1310      | This work |
| Congruent reaction  | L ↔ Th <sub>3</sub> Al <sub>2</sub>                         |      | 40        |      | 1301 ± 2  | [20]      |
|                     |   |      | 40        |      | 1300      | This work |
| Congruent reaction  | L ↔ ThAl <sub>2</sub>                                       |      | 66.7      |      | >1520     | [20]      |
|                     |   |      | 66.7      |      | 1520      | This work |

estimated values by Kassner et al. [20] is smaller than 4 at.% Al. Since there is no enough experimental data on the liquidus, this calculated result is acceptable and can provide information for the further experiment. The calculated solid solubilities of Al in the βTh and αTh phases are respectively less than 1.5 at.% and 2 at.%, which are close to Murray's result [17].

The calculated enthalpy and entropy of formation in the whole compositional region at 1000 K based on the present assessed ther-

modynamic parameters are shown in Figs. 4 and 5, which are in good agreement with the experimental data [19,21].

#### 4.2. The Th–Zn system

The calculated phase diagram in the Th–Zn system with experimental data [26] is shown in Fig. 6. The calculated phase diagram

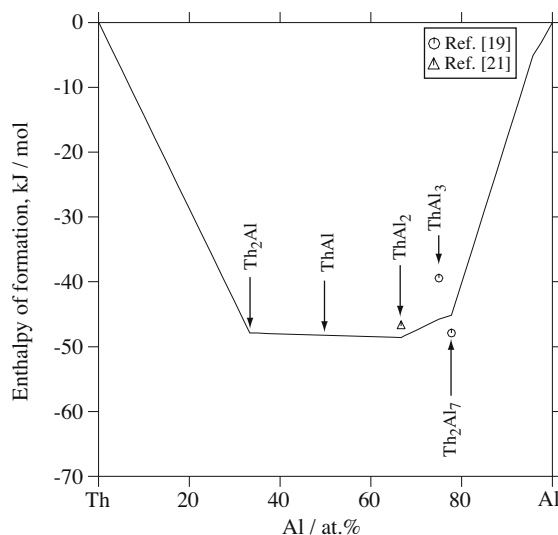


**Fig. 4.** The calculated enthalpy of formation at 1000 K in the Al–Th system compared with the experimental data [19,21]. (The reference states of pure elements of Th and Al are αTh and liquid phases, respectively.)

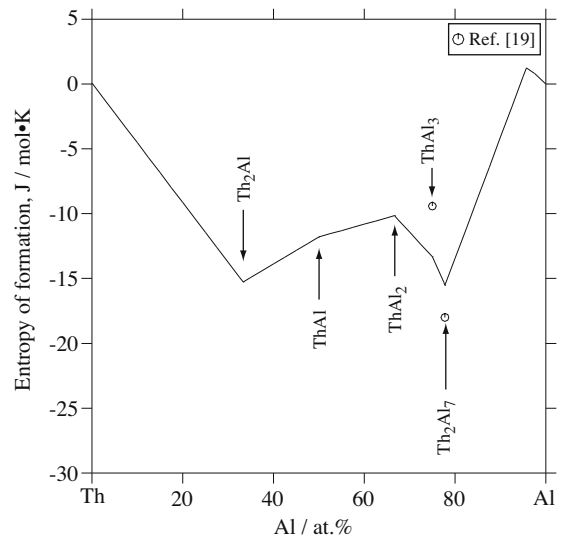


**Fig. 5.** The calculated entropy of formation at 1000 K in the Al–Th system compared with the experimental data [19]. (The reference states of pure elements of Th and Al are αTh and liquid phases, respectively.)

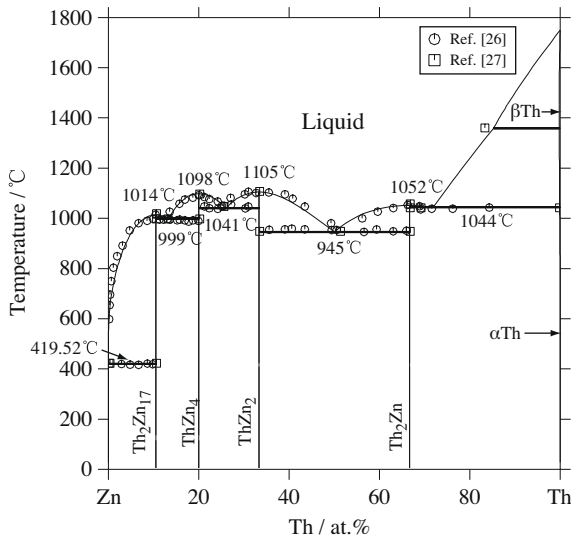


Fig. 6. The calculated phase diagram of the Th–Zn system with the experimental data [26,27].

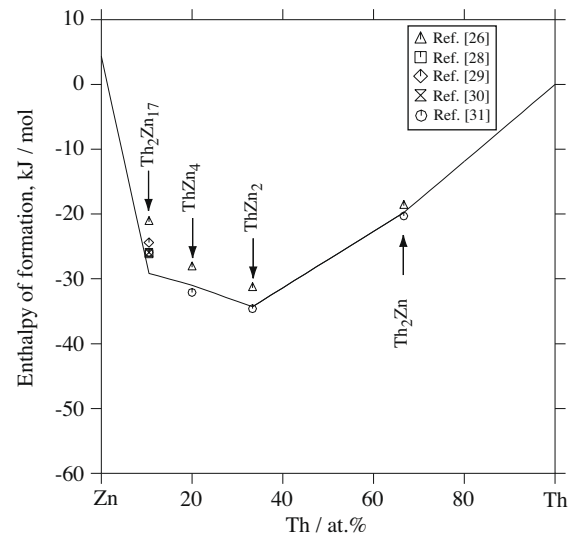


Fig. 7. The calculated enthalpy of formation at 700 K in the Th–Zn system compared with the experimental data [26,28–31]. (The reference states of pure elements of Th and Zn are  $\alpha$ Th and hcp phases, respectively.)

**Table 5**  
Experimental and calculated invariant reactions in the Th–Zn system.

| Reaction type       | Reaction   | Th (at.%) | T (°C) | Reference              |                          |
|---------------------|--|-----------|--------|------------------------|--------------------------|
| Catatectic reaction | $\beta\text{Th} \leftrightarrow \alpha\text{Th} + \text{L}$          | 100       | 100    | –                      | 1360 [27]<br>This work   |
| Eutectic reaction   | $\text{L} \leftrightarrow \alpha\text{Th} + \text{Th}_2\text{Zn}$    | 69.5      | 100    | 66.7                   | 1040 [27]<br>This work   |
| Eutectic reaction   | $\text{L} \leftrightarrow \text{ThZn}_2 + \text{ThZn}_4$             | 25.6      | 33.3   | 20                     | 1045 [27]<br>This work   |
| Eutectic reaction   | $\text{L} \leftrightarrow \text{ThZn}_4 + \text{Th}_2\text{Zn}_{17}$ | 13.2      | 20     | 10.5                   | 995 [27]<br>This work    |
| Eutectic reaction   | $\text{L} \leftrightarrow \text{Th}_2\text{Zn} + \text{ThZn}_2$      | 51.4      | 66.7   | 33.3                   | 945 [27]<br>This work    |
| Eutectic reaction   | $\text{L} \leftrightarrow \text{Th}_2\text{Zn}_{17} + (\text{Zn})$   | 0         | 10.5   | 0                      | 419.58 [27]<br>This work |
| Congruent reaction  | $\text{L} \leftrightarrow \text{Th}_2\text{Zn}$                      | 66.7      | 66.7   | 1055 [27]<br>This work |                          |
| Congruent reaction  | $\text{L} \leftrightarrow \text{ThZn}_2$                             | 33.3      | 33.3   | 1105 [27]<br>This work |                          |
| Congruent reaction  | $\text{L} \leftrightarrow \text{ThZn}_4$                             | 20        | 20     | 1095 [27]<br>This work |                          |
| Congruent reaction  | $\text{L} \leftrightarrow \text{Th}_2\text{Zn}_{17}$                 | 10.5      | 10.5   | 1015 [27]<br>This work |                          |

is in agreement with most of the experimental results reported by Chiotti and Gill [26]. In the Th-rich region, a smaller solubility of Zn in the  $\alpha$ Th and  $\beta$ Th phases was given in this work, and the liquidus in the Th-rich region was predicted according to the assessment of Chiotti and Gill [26]. These results can provide information for the further experiment. All the invariant equilibria in the Th–Zn system are listed in Table 5.

Figs. 7 and 8 show the calculated enthalpy and entropy of formation in the whole compositional region at 700 K based on the present assessed thermodynamic parameters with the experimental data [26,28–31], where the reference states of pure elements of Th and Zn are fcc and hcp phases, respectively. Good agreement is obtained between the present calculated results and experimental data [26,28–31].

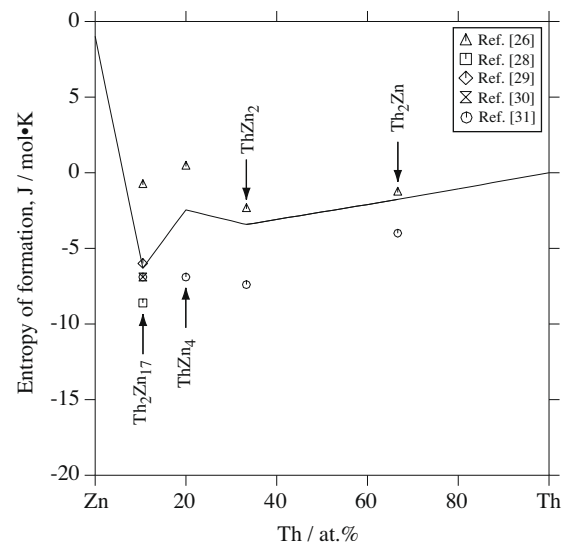


Fig. 8. The calculated entropy of formation at 700 K in the Th–Zn system compared with the experimental data [26,28–31]. (The reference states of pure elements of Th and Zn are  $\alpha$ Th and hcp phases, respectively.)

## 5. Conclusions

The phase diagrams and thermodynamic properties in the Al–Th and Th–Zn binary systems were evaluated from the available experimental information in literature. A consistent set of optimized thermodynamic parameters has been derived for describing the Gibbs free energy of each solution phase and intermetallic compounds in the Al–Th and Th–Zn binary systems. Most of experimental information can be satisfactorily reproduced on the basis of the optimized thermodynamic parameters.

## Acknowledgements

This work was supported by the National Natural Science Foundation of China (Nos. 50425101, 50771087, 50725413), the

Ministry of Education, PR China (No. 707037), and the National Basic Research Program of China (No. 2007CB613704).

## References

- [1] D.J. Hill, *Nat. Mater.* 7 (2008) 680.
- [2] R.W. Grimes, R.J.M. Konings, L. Edwards, *Nat. Mater.* 7 (2008) 683.
- [3] C. Guéneau, S. Chatain, S. Gossé, C. Rado, O. Rapaud, J. Lechelle, J.C. Dumas, C. Chatillon, *J. Nucl. Mater.* 344 (2005) 191.
- [4] J. Stephen Herring, P.E. MacDonald, K.D. Weaver, *Nucl. Eng. Des.* 203 (2001) 65.
- [5] J. Wang, C.P. Wang, X.J. Liu, *J. Nucl. Mater.* 374 (1–2) (2008) 79.
- [6] C.P. Wang, P. Yu, X.J. Liu, I. Ohnuma, R. Kainuma, K. Ishida, *J. Alloys Compd.* 457 (1–2) (2008) 150.
- [7] J. Wang, X.J. Liu, C.P. Wang, *J. Nucl. Mater.* 380 (1–3) (2008) 105.
- [8] X.J. Liu, Z.S. Li, J. Wang, C.P. Wang, *J. Nucl. Mater.* 380 (1–3) (2008) 99.
- [9] C.P. Wang, Y.F. Li, X.J. Liu, K. Ishida, *J. Alloys Compd.* 458 (1–2) (2008) 208.
- [10] Z.S. Li, X.J. Liu, C.P. Wang, *J. Alloys Compd.* 476 (1–2) (2009) 193.
- [11] C.P. Wang, W. Fang, Z.S. Li, X.J. Liu, *J. Nucl. Mater.* 392 (3) (2009) 525.
- [12] A.T. Dinsdale, *Calphad* 15 (1991) 317.
- [13] O. Redlich, A.T. Kister, *Ind. Eng. Chem.* 40 (1948) 345.
- [14] A. Leber, *Z. Anorg. Chem.* 166 (1927) 16.
- [15] G. Grube, L. Botzenhardt, *Z. Elektrochem.* 48 (1942) 418.
- [16] H.A. Saller, F.A. Rough, *Compilation of US and UK Uranium and Thorium Constitutional Diagrams*. USAEC Rept., BMI-1000, 1955.
- [17] J.R. Murray, *J. Inst. Met.* 87 (1958) 349.
- [18] G.H. Bannister, J.R. Thomson, *J. Nucl. Mater.* 12 (1964) 16.
- [19] A.M. Poyarkov, V.A. Lebedev, I.F. Nichkov, S.P. Raspopin, *Sov. Atom. Energy* 35 (1973) 1138.
- [20] M.E. Kassner, D.E. Peterson, *Bull. Alloy Phase Diag.* 10 (1989) 466.
- [21] J.W. Wang, Q.T. Guo, O.J. Kleppa, *J. Alloys Compd.* 313 (2000) 148.
- [22] E.S. Makarov, S.I. Vinogradov, *Kristallografiia* 1 (6) (1956) 634.
- [23] E.S. Makarov, L. Gudkov, *Kristallografiia* 1 (6) (1956) 650.
- [24] N.C. Baenziger, R.E. Rundle, A.L. Snow, *Acta Cryst.* 9 (1956) 93.
- [25] M.V. Smimov, N.G. Ilyushchenko, S.P. Detkov, L.E. Ivanovskii, *Zhur. Fiz. Khim.* 31 (1957) 1013.
- [26] P. Chiotti, K.J. Gill, *Trans. AIME* 221 (1961) 573.
- [27] H. Okamoto, *Desk Handbook-Phase Diagrams for Binary Alloys*, ASM International, 2000.
- [28] Yu.P. Kanashin, V.A. Lebedev, I.F. Nichkov, S.P. Raspopin, *Izv. Akad. Nauk. SSSR, Met.* 3 (1972) 46.
- [29] P. Chiotti, M. Koizumi, Report IS-193 (Ames Laboratory, Ames, IA), 1960, p. 32.
- [30] P. Chiotti, C.H. Dock, *J. Less-Common Met.* 41 (1975) 225.
- [31] P. Chiotti, V.V. Akhachinskij, I. Ansara, *The Chemical Thermodynamics Of Actinide Elements Compounds, part 5: The Actinide Binary Alloys*, in: V. Medvedev, M.H. Rand, E.F. Westrum Jr., F.L. Oetting (Eds.), International Atomic Energy Agency, Vienna, 1981.
- [32] J.O. Andersson, T. Helander, L. Höglund, P.F. Shi, B. Sundman, *Calphad* 26 (2002) 273.